



Scour depth estimation in a balanced cantilever bridge with deteriorated central hinges based on natural frequencies: field measurements, methodology for estimation and verification

M. S. I. Choudhury¹ · Y. Matsumoto¹ · A. F. M. S. Amin²

Received: 15 March 2018 / Accepted: 6 August 2018 / Published online: 14 August 2018
© Springer-Verlag GmbH Germany, part of Springer Nature 2018

Abstract

A scheme based on field measurements of vibrations is proposed for estimating the scour depths of a multi-span balanced cantilever bridge resting on foundations embedded in soft soil. Field measurements of ambient vibrations using velocity sensors indicated elongated periods of vibration in the transverse direction at the pier tops due to scour underneath. The modal properties were identified using the Eigensystem Realization Algorithm. The unknown spring constants of the central hinges were determined to represent the deteriorated performance of the bridge superstructure under no-scour benchmark conditions from a finite element model incorporating soft soil conditions. A single set of spring constants compatible with the measured natural frequencies was thus identified for the transverse movement of the central hinges. The strong dependence of the transverse bending mode of the pier and weak dependence of the longitudinal bending mode of the pier on scour phenomena were clearly observed. The observed relationships between the scour depth and natural frequency were sensitive to soft soil conditions in both modes. The estimated spring constants representing soft soil were used to assess the unknown scour depths in the pier foundations suffering from scour. Independent bathymetric surveys verified the general applicability of the proposed scheme for estimating the scour depths around bridges of this type within reasonable limits.

Keywords Scour · Balanced cantilever bridge · Central hinge · Natural frequency · SHM · Soft soil

1 Introduction

Scour, which constitutes the local removal of riverbed material around a foundation due to water flow, is an important consideration in the design, operation and maintenance of bridges constructed over water bodies (see, e.g., [1–3]). Alluvial rivers that flow from the great

Himalayan range that form the Bengal Basin [4–7] are known for inducing significant scour effects around the foundations of hydraulic structures (see, e.g., [8]). Scour particularly affects foundations in riverbeds (which typically comprise thick strata composed of fine-grained sediments) in these types of active river basins susceptible to atypically large hydraulic loads through high-velocity turbulence. In an optimal design, the safety of bridge foundations can be assured by either reducing the size of the foundations to reduce flow disturbance or increasing the foundation embedment depth (see, e.g., [9, 10]). However, a reduction in the foundation size also shortens the bridge span, and increasing the foundation depth often leads to restrictions associated with the limits of practical construction. Accordingly, the construction of balanced cantilever bridges (Fig. 1) with short and medium spans is common throughout the Bengal Basin [11]. The installation of a mechanical hinge joint (Fig. 1a) at the center of a balanced cantilever span, also known as the central hinge

✉ M. S. I. Choudhury
sichow00@gmail.com

Y. Matsumoto
ymatsu@mail.saitama-u.ac.jp

A. F. M. S. Amin
samin@ce.buet.ac.bd

¹ Department of Civil and Environmental Engineering,
Saitama University, Saitama-Shi, Saitama 338-8570, Japan

² Department of Civil Engineering, Bangladesh University of
Engineering and Technology, Dhaka 1000, Bangladesh

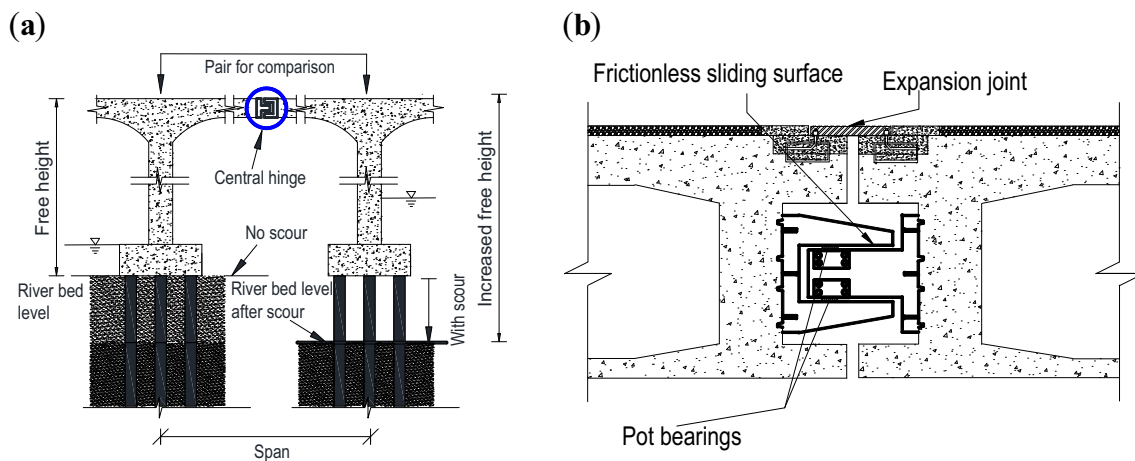


Fig. 1 The effect of scour on the global dynamic behaviors of balanced cantilever bridges with a central hinge (shown schematically). **a** A bridge with a central hinge. **b** Details of a typical central hinge joint

([12]; Fig. 1b), is often economical for the construction of longer spans. The deflections and rotations induced by static forces and time-dependent forces are accommodated by two pot bearings at that joint. Consequently, such bridges require regular monitoring in terms of the performance of the central hinge and the scour depth [13, 14] to satisfy the necessary design conditions during their service life.

However, endeavors to repair and rehabilitate the Meghna Bridge (see also Sect. 2) and the Gumti Bridge in Bangladesh and the Yamuna Bridge in Kalpi, India, have been extensive, time-consuming and often repetitive [11, 12, 15–19]. These repairs have, on several recent occasions, involved unavoidable bridge closures in busy corridors because insufficient information was known about the deteriorated performance of the central hinges. Furthermore, scour often remains either undetected or unassessed. The evolution of scour around foundations increases the flexibility of the structures as a consequence of the increase in the free height, leading to elongated periods of vibration (see also [20, 21]) that could greatly threaten the fatigue life. To ensure safe operations and reduce maintenance efforts for this class of bridges that are currently in service, the development of a simple scheme to compare the natural frequency (f) with benchmark data involving changes in the free height due to scouring (c.f. [22] and the references cited therein) in soft soil and to characterize the condition of the central hinge would be extremely valuable. Using such a scheme, decisions could be made in regard to initiating time-critical maintenance when safe access to piers is impossible during peak monsoon flows (e.g., through traditional bathymetric surveys or visually inspecting the foundations by deploying divers for free height assessment) due to strong currents and turbulence [23]; other remote sensing measures also possess

their own advantages and disadvantages [13, 14, 23–27]. In this way, the possibility of sudden and catastrophic bridge failure due to scour [13, 14, 21, 28–33] can perhaps be reduced.

In this regard, a novel idea for applying such devices to estimate the scour depth is presented here based on the wide availability of portable vibration-based sensors suitable for gathering field data under all-weather conditions. At approximately the same time that the research described in this paper began, Foti and Sabia [34] proposed concepts for scour monitoring based on the acquisition of data from versatile vibration sensors installed at designated locations on existing simply supported, pre-stressed reinforced concrete bridges resting on piers to observe the structural system's dynamic responses. The measurement results were compared with the simulations of finite element (FE) models for various foundation embeddings in 'no-scour' and 'with-scour' scenarios. In addition, Elsaied and Seracino [35] reported the effects of scour on the movements of a bridge deck without any underwater instrumentation using a scaled laboratory model of a two-span continuous bridge. Furthermore, Lin et al. [36] investigated the effects of scour with different water levels on the structural dynamic characteristics in a scaled laboratory experiment with an independent single-pier model set in an indoor water channel. It was reported that the embedment depth of the bridge column has a primary effect on the natural frequency rather than the water level. Subsequently, Chen et al. [37] proposed a scour evaluation method for the foundation of a cable-stayed bridge based on ambient vibration measurements of the superstructure; the importance of considering the soil stiffness was credited to Lin et al. [36]. In contemporary contribution, Zarafshan et al. [38] reports the change in frequency of vibration of a driven rod system to detect the presence of scour. A

computational methodology was proposed employing Winkler spring reaction model for soil (c.f. [39] and the references cited therein) to calibrate the developed system for a riverbed. The system was tested both in laboratory and field to detect and measure scour through change in vibration frequency of rod due to increase in its cantilevered length (free height, Fig. 1, see also [40]). Analytical approaches based solely on numerical models have also been used to theoretically investigate the effects of scour on the dynamic properties of simply supported bridges, as seen in Ju [41], Zheng and Yu [31], Feng et al. [42], Prendergast et al. [20, 21], and Kong and Cai [43]; however, these researchers assumed ideal joint and bearing behaviors. Moreover, early reports of vibration measurements [34, 35] were not sufficiently elaborate to include the joint performance in the assessment procedure. Nevertheless, to obtain a reasonable assessment of the scour depth, it is necessary to consider the interactions among the various components of the substructure and superstructure of a bridge using a rational model, wherein the behaviors of the joints and the fixity of the foundation under field conditions are adequately represented in the model based on the field conditions. The dynamic dependencies between each component, which can vary widely among the bridge forms [37], must be considered in any scour depth assessment scheme.

Moreover, when no theoretical or field verification has been performed, it is worthwhile to confirm the influences of the deep, soft soil strata considered in the model on the estimated scour depth using a vibration-based approach (see Prendergast et al. [21, 44], Feng et al. [42], Chen et al. [37] and Kong and Cai [43] for hard soil types, which result in less foundation flexibility than the soft soil types [45] encountered in the Bengal Basin, which can lead to substantial scour). Wang et al. [13] noted that scour depth estimates using dynamic properties obtained from field measurements of the vibrations of bridge superstructures remain in their infancy because their sensitivity and reliability in regard to scoured soil-pier behaviors (which should be different between hard soil and soft soil types) lack direct field validation. The absence of any such approach forces maintenance engineers to use either bathymetric measurements of riverbed profiles (often containing loose rubble exhibiting less active confinement of the foundation) and to conduct inspections away from the bridge piers or to wait until the next dry season, thereby leaving the bridge under threat of scour. However, the actual fixed location of the embedded foundation offered by the confined soil strata [8] under scour remains unevaluated [18].

In consideration of the above background, ambient vibration measurements were taken using velocity sensors at the pier tops and central hinges of the 13-span, 930-m-

long Meghna Bridge, a pre-stressed concrete (PC) box girder balanced cantilever bridge resting on soft soils in the alluvial fan of the Bengal Basin in Bangladesh. The measurements were collected under normal rainy season flooding conditions during the active southwest monsoon without any underwater instrumentation. Measurements were obtained at the scour-prone outer bank spans and compared with the benchmarks. The natural frequencies of the dominant modes were identified by applying the Eigensystem Realization Algorithm (ERA [46]) to the acquired data. The effects of the soil conditions were considered in an FE model developed with general purpose software [47] using the parameters estimated from the bore logs [45]. To separate the scour effects from the performances of the bridge and central hinge, benchmark measurements were utilized to assess the unknown spring constants of the deteriorated central hinges. The determined spring constants were applied to derive an estimate of the scour depth from the relationship between the natural frequency and the scour depth in the vibration modes that are sensitive to scour. Bathymetric survey data collected simultaneously and away from the bridge centerline were utilized for independent verification.

2 Scour and vibration of the Meghna Bridge

The basic geometry of the Meghna Bridge extracted from the original design report and drawings is illustrated in Fig. 2 [45]. Throughout its service life following its construction from 1987 to 1991, the Meghna Bridge has presented a historic problem of scour around its outer bank pier foundations (Fig. 2a). Furthermore, each of the central hinges (see also Fig. 1) for the nine river spans of the bridge has deteriorated during its service life due to a lack of maintenance [11, 15, 17, 18]. Moreover, there are no records about the maintenance or monitoring performed on the bridge. Consequently, it is prudent for the authors to utilize field vibration data at certain locations on the piers of this bridge with scour holes to estimate the scour depth below the pile cap (Fig. 2b, d) by taking advantage of the symmetry of the bridge geometry and the asymmetry at the scour locations (Fig. 2a).

2.1 Advantages of the geometrical symmetry in the study

The symmetrical geometries (Fig. 2a) of the bridge spans and the pier heights (between piers P1 and P10 about the central hinge at E5 along a distance of 783 m of its total length of 930 m) above the pile caps together with the fact that scour features are located only around the outer bank piers result in unique pairs of conditions (i.e., ‘no-scour’

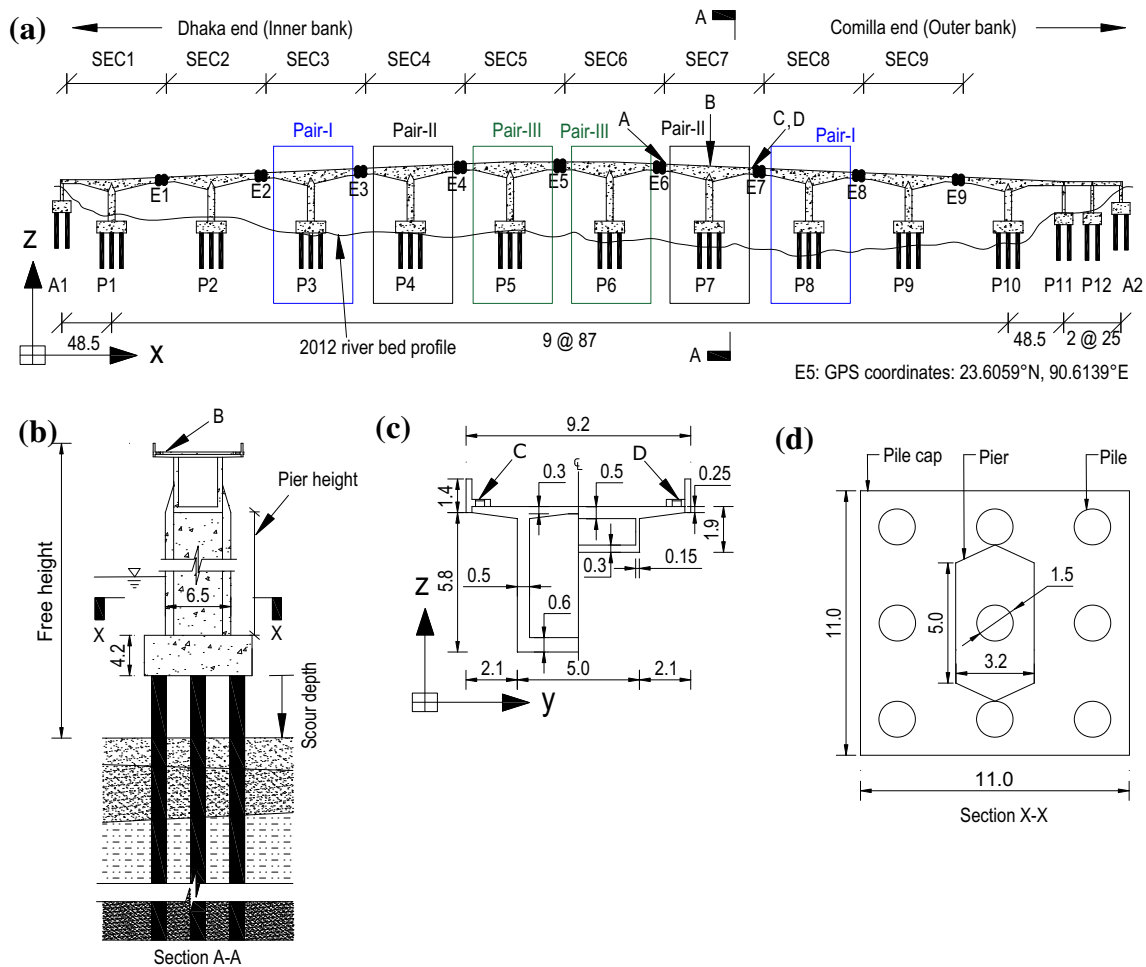


Fig. 2 Geometric configuration of the Meghna Bridge. **a** Schematic elevation, where EX: expansion joint and central hinge at location X, AY: abutment at location Y, PZ pier at location Z, and A, B, C and D: typical sensor locations for a typical river span. Three pairs, namely,

and ‘with-scour’ scenarios), thereby facilitating a comparative assessment of the applicability of this approach with its utility for more general cases encountered elsewhere (first assumption). To investigate the effects of scour on the natural frequency of the bridge structure, three pairs were selected based on the equivalent structural forms of the sections (SECs). Pair-I, which consisted of SEC3 (no-scour) and SEC8 (with-scour); Pair-II, which consisted of SEC4 (no-scour) and SEC7 (with-scour); and Pair-III, which consisted of SEC5 (no-scour) and SEC6 (with-scour), were selected for the analysis (see also Fig. 3). The terms, e.g., scour depth, pier height and free height (the embedment depths under ‘no-scour’ and ‘with-scour’ conditions), mentioned throughout the paper, are illustrated in Fig. 2b. The geometric properties of the box girder, pier and pile caps are shown in Fig. 2c, d and used to develop the FE model (Sect. 3). Furthermore, in the assessment, the limiting behaviors of the hinges for each of the pairs can be

Pair-I, Pair-II and Pair-III, are selected based on the symmetry of the superstructure. **b** Scour depth, pier height and free height in section A-A (see also Tables 1 and 2). **c** Box girder cross section. **d** Section X-X shows the top view of the pile foundation

assumed to be similar based on the symmetry of the bridge (second assumption).

2.2 Soil profile and scour

The soil profiles along the centerline of the bridge at each of the pier locations P3 through P8, which are relevant to this study, are shown in Fig. 3. The bore logs [45] show the existence of soft materials down to depths of 40 m. The top three layers of soil with thicknesses from approximately 15 m to 18 m at the different piers consisted of sand. The middle portion of the soil consisted of a layer of silty soil approximately 15 m thick. The remaining soil layers consisted of very dense sandy soil to very dense sand. The modulus of deformation for each of the different soil layers (Sect. 3) beneath the Meghna Bridge was calculated from the standard penetration test (SPT) values for each of the pier locations (Fig. 3).

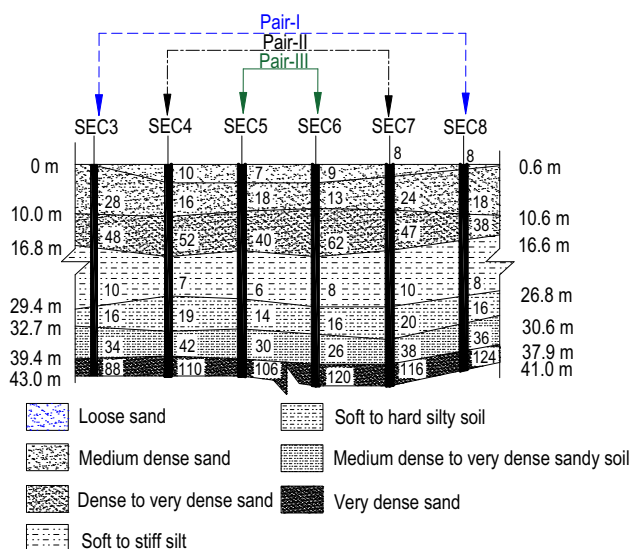


Fig. 3 The soil profiles at different SECs along the Meghna Bridge. Standard penetration test (SPT) values are also shown. The pile cap bottom is the datum. Three pairs, namely, Pair-I, Pair-II and Pair-III, represent the comparisons between the locations SEC3 and SEC8, SEC4 and SEC7, and SEC5 and SEC6, respectively, based on the ‘no-scour’ benchmark and ‘with-scour’ conditions. The nomenclatures and notations used throughout the paper are also given in Fig. 2

Minimal documentation is available for the scour around the Meghna Bridge because of the presence of sustained turbulence around the pier holes. The scour depths at the foundations of the piers could never be documented due to this turbulence; instead, they have been sensed through bathymetric measurements away from the piers, strongly warranting the application of an alternative and more reliable method. Meanwhile, a conservative modification to the original hydraulic design was subsequently adopted for P6–P9 to account for hydraulic loads that were more severe than expected during the construction [48]. Stone pitched collars (falling aprons) were constructed for deployment upon the initiation of scour at the toe of the apron [49–51]. As a result, the locations of scour phenomena shifted away from the pier foundations. This deployment increased the free height (Fig. 2b) due to a decrease in the effective confinement as the bed materials below the apron were lost due to scour. Repeated mitigation efforts were subsequently necessary to protect the aprons. Finally, three different organizations (Survey-I, Survey-II and Survey-III)

reported scour depths at P6, P7 and P8 after performing bathymetric surveys using an echo-sounding technique in 2012; those scour depths form the basis of the current study. The measurements varied with the distance from the bridge centerline (see also Fig. 14), and the average scour depths estimated from Survey-I, Survey-II and Survey-III are summarized in Table 1. These recorded scour depths are used in Sect. 8 to independently verify the proposed vibration-based scheme and discuss the results objectively. Table 2 summarizes the pier heights and the increases in the free heights (based on bathymetric survey) at P6, P7 and P8 (under ‘with-scour’ conditions) compared with those at P5, P4 and P3 (under ‘no-scour’ conditions).

2.3 Central hinge performance

At the time when the ambient vibration measurements were acquired, the states of the pot bearings of the central hinges (Fig. 1a, b) significantly deviated from an ideal state due to excessive traffic loading and insufficient maintenance. Much of the rubber cushion inside the pot bearings suffered from aging, wear and tear, creating gaps between the pot bearing surface and the frictionless sliding surfaces at the hinge joints (Fig. 1b, Table 3). This deterioration of the central hinges transformed the bridge into a ‘true’ balanced cantilever section through the creation of these gaps and created free cantilever ends. Moreover, the direct transfer of the vertical force by the hinges at the cantilever end occurs only after the displacement/rotation exceeds the gap during vibration. To account for this, two different boundary conditions were used in the FE model, and the outputs of the vibration records were matched to ascertain the actual phenomena (i.e., free conditions or closed conditions) occurring at the time of taking the measurements (Sect. 3).

3 Methodology for estimating the scour depth

No underwater instruments were used to estimate the scour depth in contrast to Gorin and Haeni [23], Hayes and Drummond [25], Millard et al. [26] and De Falco and Mele [27]. Furthermore, fewer sensors (4 sensors on the

Table 1 Scour depths measured using echo-sounders [52]

	Scour depths, m					
	SEC8		SEC7		SEC6	
	Min.-max.	Mean	Min.-max.	Mean	Min.-max.	Mean
Survey-I	9.5–15.8	11.0	5.8–11.8	6.4	–	–
Survey-II	10.5–11.6	11.13	5.0–8.5	6.5	–	–
Survey-III	9.5–14.5	12.0	3.6–9.75	6.7	2.6–5.6	4.1

Table 2 Pier heights and free heights under “with-scour” conditions

Pair	Pier/SEC	Pier height (m)	Free height (m)
Pair-I	P3/SEC3	24.7	34.7
	P8/SEC8		45.8
Pair-II	P4/SEC4	27.0	36.9
	P7/SEC7		43.4
Pair-III	P5/SEC5	29.2	39.0
	P6/SEC6		43.1

Table 3 Gaps measured between the top and bottom surfaces of pot bearings and frictionless sliding surfaces under neutral conditions (i.e., when the bridge is not in service)

Central hinge	E2	E3	E4	E5	E6	E7	E8	E9
Gap (mm)	55	60	57	60	60	65	65	65

The averages of the top and bottom gaps are documented in this study for each of the central hinge locations

deck, Fig. 2a) than were used by Foti and Sabia [34] or Chen et al. [37] were employed on the bridge deck to estimate the scour depth. Symmetric pairs of piers (Sect. 2.1) were used as a benchmark for the first time to estimate the scour depth of a real scoured balanced cantilever bridge with deteriorated central hinges based on the vibration data. For real balanced cantilever bridges with deteriorated central hinges and scour phenomena, the sensitivity of the natural frequency to scour is not fully known, and there is a lack of evidence that can be utilized to estimate the scour depth. Therefore, a framework for estimating the scour depth from the natural frequency was investigated in this study.

A schematic representation of the methodological framework implemented for the estimation of the bridge scour depth

as an advancement in structural health monitoring (SHM) is shown in Figs. 4 and 5. The outcomes of this study following the methodology proposed herein are presented in Sects. 4, 5, 6 and 7. Additionally, the scour depths estimated from the vibration records following the proposed methodology are verified and discussed with independent bathymetric survey results (Table 1) in Sect. 8.

3.1 Consideration of physical conditions

A reliable FE model representing the actual conditions of a bridge in service is required as a baseline for comparison. To build such a model, the effects of wear and tear (i.e., effects on the stiffness of the girder, pier, foundation and end conditions at the hinge locations) on the bridge must be based on physical visual inspections. Based on the gaps observed in the central hinges (Table 3), the boundary conditions for both ends of the cantilever portions of each SEC need to be addressed for two separate instances: (i) free conditions when the gap is open due to low-amplitude vibrations, and (ii) closed conditions when the gap is transiently closed after the net displacement due to vibration exceeds the gap value (Table 3). The stiffness of the superstructure will be lower in the open state than in the closed state due to contact between adjacent surfaces and the subsequent transmission of the vertical force. In the first analysis case, the boundary conditions in the model were free, thereby representing each SEC as an isolated SEC. FE modal analysis was performed for each SEC under ‘no-scour’ benchmark conditions, and the foundations affected by scour were identified through comparison with the measurements. In the second case, when vibrations occurring at a higher amplitude close the gap (Table 3), the highly nonlinear phenomena occurring in three dimensions need to be considered ideally in the model to represent the

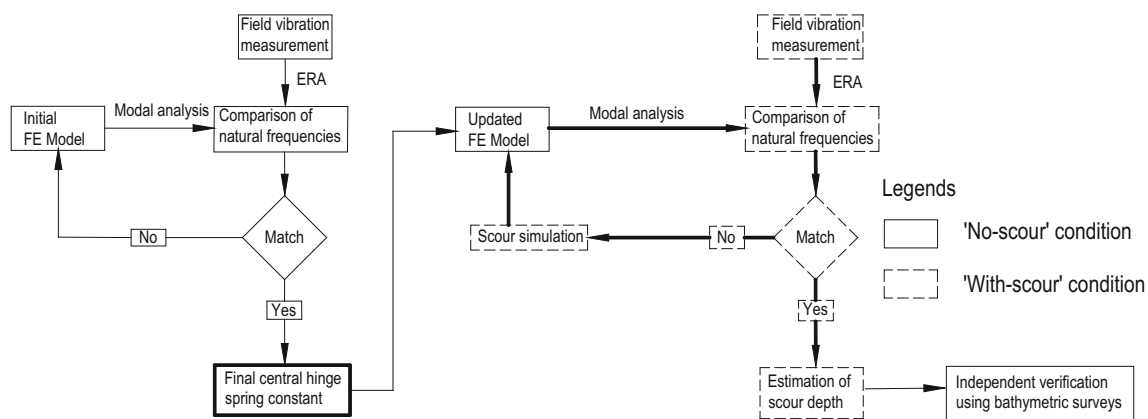


Fig. 4 Scour depth estimation scheme for each of the pier locations. The matching scheme for estimating the compatible central hinge spring constants and the obtained values are illustrated in Fig. 5

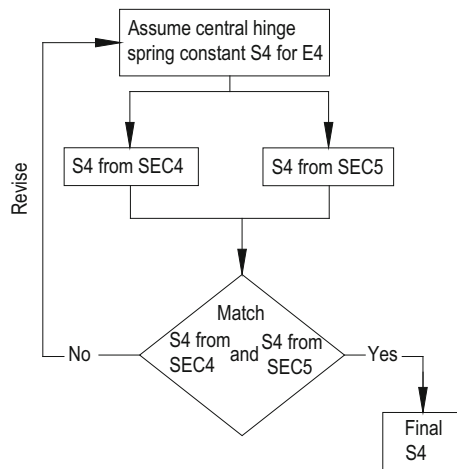


Fig. 5 Flow chart for the matching scheme to estimate the central hinge spring constants in the y-direction. Sample spring constant estimation flow chart, where S4 denotes the spring constant for E4, as an example

actual physical condition. For the sake of simplification to meet the specific objectives of this study, linear springs were assigned at both ends of the cantilever portion of each SEC to account for the effects of adjacent sections in the modal analysis of a section. However, the spring constants of damaged central hinges are unknown. Therefore, the FE models must be tuned with a unique stiffness value compatible with the vibration measurements representing the actual field conditions. Furthermore, under ideal conditions, the movement of the bridge in the y-direction (transverse direction or direction of river flow) is restricted, and relative movement in the x-direction (longitudinal direction or direction of car movement) is allowed within a certain limit based on the limit of the central hinges (Fig. 2). However, due to the severe damage to the pot bearings, these ideal movements are affected when transferring the vertical (z-direction) load. Consequently, to quantify the movements of individual sections at the central hinge locations, springs are also assigned to the y-direction in the model. Thus, the y-direction is used in this study (see Sect. 7.1 for the results) to estimate the scour depth based on Feng et al. [42], Ju [41] and Elsaid and Seracino [35] in contrast to Prendergast et al. [21], who considered the x-direction. Springs in the x-direction and z-direction represent the longitudinal and vertical restraints, respectively.

3.2 Outline of the scheme

The scour depth estimation scheme for each pier location is shown in Fig. 4. The natural frequencies obtained from the FE model through modal analysis were compared with the natural frequencies identified from field vibration records

through the ERA [46] under the ‘no-scour’ benchmark condition. The spring constants were estimated for the central hinges under the ‘no-scour’ condition (for SEC3, SEC4 and SEC5) by matching the natural frequencies obtained from the FE model with those from field measurements using the scheme shown in Fig. 5. The presented flow chart schematically represents the connection of E4 with SEC4 and SEC5 (Fig. 5), as an example case. This approach taking only two segments and one central hinge with the y-direction stiffness at a time greatly reduces the need to address the unknowns of all central hinges simultaneously. The estimated spring constants for the central hinges under the ‘no-scour’ condition were used in the FE model for SEC6, SEC7 and SEC8 under ‘with-scour’ conditions, and a comparison was performed between the natural frequencies obtained from the FE analysis and ERA (Fig. 4).

3.3 FE model for representing the bridge geometry and soft soil conditions

The FE model of the different SECs of the Meghna Bridge was developed using the ANSYS software [47] to interpret the measurement results (Fig. 6). The geometry, soil profile, material properties and boundary conditions of the bridge were considered realistically in the model with the objective of deriving reasonable numerical results.

Young’s moduli of the concrete were 2.753×10^7 kN/m² for the deck and box girder, 2.279×10^7 kN/m² for the pier and 2.549×10^7 kN/m² for the pile. The density of the concrete was 2403 kg/m³, and Poisson’s ratio was 0.2. The single-cell, variable-depth continuous PC box girder of the rigid frame (Fig. 2c) was modeled using FEs. The BEAM188 element [47] was used to model the deck and box girders (Fig. 2c) in addition to the pier. The variations in the cross sections of the bridge piers (6.5 m × 3.2 m for P2–P9; 6.5 m × 2.7 m for P1 and P10; Fig. 2d) were considered in the model. Piles with lengths from 40 to 45 m and a diameter of 1.5 m were modeled using the BEAM188 element. The variation in the thicknesses of the pile caps with cross-sectional areas of 11.0 × 11.0 m² (between 4.2 m at the center and 3.7 m at the edge for SEC3 and SEC8 and between 4.0 m at the center and 3.5 m at the edge for SECs 4–7; see Fig. 2d) was modeled using the SOLID185 element [47].

The BEAM188 element is described as a 3D linear finite strain beam element which is capable to include shear-deformation effects [47]. The BEAM188 element is defined by two nodes in 3D having six degrees of freedom at each node, i.e., three translational degrees of freedom in the x-, y- and z-directions and three rotational degrees of freedom about the x-, y- and z-axes. The pile cap was modeled as a SOLID185 element, which is an eight-node

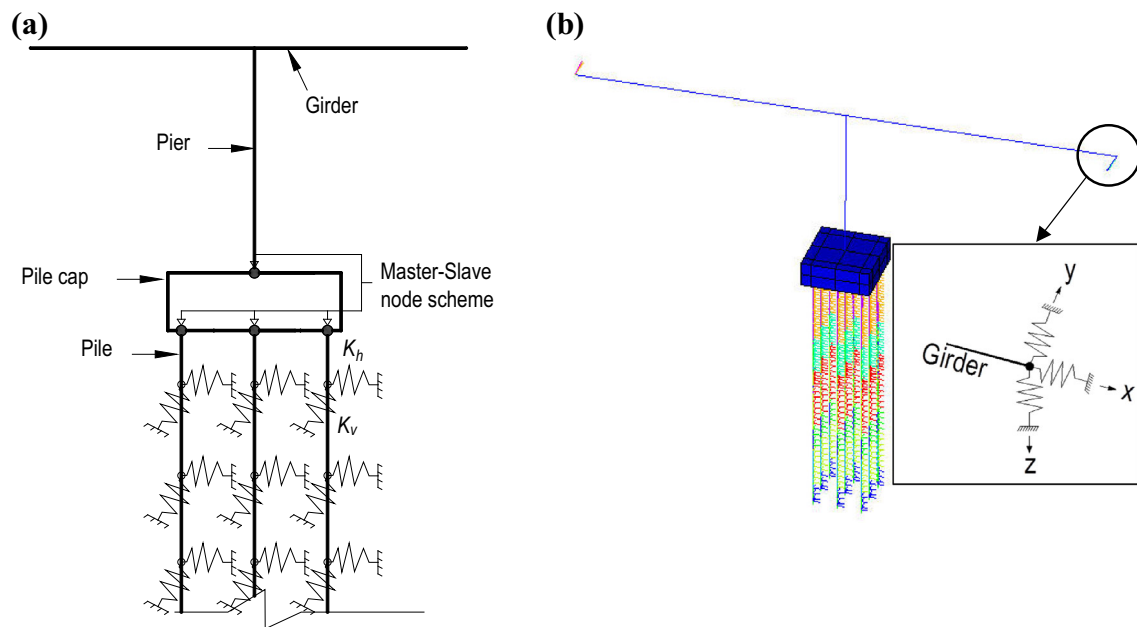


Fig. 6 Soil profile along with central hinge arrangement in the FE model. **a** Schematic representation of the soil spring elements and structural elements, where k_h represents the horizontal spring stiffness and k_v represents the vertical spring stiffness. The soil profiles at

3D structural solid element having three translational degrees of freedom in the x -, y - and z -directions at each node [47]. To create a rigid region among the pier, pile cap and pile, a master–slave node scheme, which connects elements with different degrees of freedom, was used. In this study, the BEAM188 elements (with translational and rotational degrees of freedom) were coupled with the SOLID185 elements (with translational degrees of freedom) to transmit the beam’s rotation into the solid parts of the structure, thereby preventing rigid body motion.

To model the soil layers, soil springs were considered around the piles according to their depths (Fig. 6) using Winkler model [39] in an approach similar to Zarafshan et al. [38], Lin et al. [36], Chen et al. [37] and Prendergast et al. [21, 40, 44, 53]. In this study, for the sake of simplicity while ensuring reasonable accuracy, soil springs were placed at an interval of 0.5 m based on the thicknesses of the soil layers. The soil spring constant of each soil layer was determined based on the SPT value (Fig. 3). The calculation of the modulus of the horizontal subgrade reaction for the pile foundation shown below from Eqs. (1)–(7) is based on the formulations of the Japan Road Association [54] and also recommended in Feng et al. [42].

First, the modulus of deformation of each different soil layer was calculated by the empirical Eq. (1):

$$E_0 = 2800N, \quad (1)$$

where E_0 is the modulus of deformation of soil (kN/m^2) and N is the SPT value of the soil layer. Then, the modulus

different SECs shown in Fig. 3 were used to derive the spring constants. **b** Typical FE model considering central-hinge and soil-structure behaviors

of the horizontal subgrade reaction was calculated based on the following empirical Eq. (2):

$$k_H = k_{H0} \left(\frac{B_H}{0.3} \right)^{\frac{3}{4}}, \quad (2)$$

where k_H is the modulus of the horizontal subgrade reaction (kN/m^3) and k_{H0} is the coefficient of the horizontal subgrade reaction (kN/m^3) corresponding to the value obtained by a plate bearing test with a rigid disk of diameter 0.3 m. k_{H0} was evaluated in terms of the modulus of deformation of soil by Eq. (3):

$$k_{H0} = \frac{1}{0.3} \alpha E_0, \quad (3)$$

where α is the coefficient of the subgrade reaction and α is unity under ordinary conditions. B_H is the equivalent loading width of the foundation (m), and it can be obtained via Eqs. (4) and (5):

$$B_H = \sqrt{\frac{D}{\beta}} \quad (\text{for a pile foundation}) \quad (4)$$

$$B_H = \sqrt{BD} \quad (\text{for a pile cap}), \quad (5)$$

where D is the diameter of the pile or the thickness of the pile cap (m), B is the length of the pile cap (m), and β is the characteristic value of the foundation (m^{-1}) calculated by Eq. (6):

$$\beta = \sqrt[4]{\frac{k_H D}{4EI}}, \quad (6)$$

where EI is the flexural stiffness of the foundation ($\text{kN}\cdot\text{m}^2$).

After substituting β , B_H and k_{H0} in Eq. (1) through Eq. (6), the following equation can be obtained for the horizontal subgrade reaction modulus of the pile foundation:

$$k_H = 1.208E_0^{1.103} \left(\frac{\sqrt{EI}}{D} \right)^{\frac{-6}{29}} \quad (7)$$

For the pile foundations of the Meghna Bridge, with E , I and D values of $2.549 \times 10^7 \text{ kN/m}^2$, 0.249 m^4 and 1.5 m , respectively; Eq. (7) can be expressed as follows:

$$k_H = 0.260E_0^{1.103} \quad (8)$$

The horizontal spring constants (k_h) were calculated based on the k_H profile, and the average end area formula [55] can be expressed as follows:

$$K_{h,i} = \frac{BL}{6} (2k_{H,i} + k_{H,i-1}) \text{ or } \frac{BL}{6} (2k_{H,i} + k_{H,i+1}), \quad (9)$$

where B is the projected pile width (m), L is the nodal spacing (m), $k_{H,i}$ is the modulus of the horizontal subgrade reaction at the i th node (kN/m^3), and $K_{h,i}$ is the horizontal spring constant at the i th node (kN/m).

The vertical spring constants along the surfaces of the piles were calculated based on the following formula:

$$K_{v,i} = \frac{K_{h,i}}{2(1 + \nu_D)} \left(\frac{\pi}{2} \right), \quad (10)$$

where $K_{v,i}$ is the vertical spring constant at the i th node (kN/m) and ν_D denotes Poisson's ratio of the soil.

The COMBIN14 linear element [47] was used to model the soil; this element is defined by two nodes, and it constitutes a uniaxial tension–compression element with up to three degrees of freedom at each node.

3.4 Field measurements

Four triaxial velocity sensors oriented along the three axes (x , y and z -axes, Fig. 2) were used for each measurement. Only one SEC was considered at a time (Fig. 2a). These sensors were placed along the bridge curbs with a distance of 43.5 m between two adjacent observation points (Fig. 2a). The sensors were placed on a device with a weight of approximately 5 kg equipped with three adjustable nuts used to adjust the horizontal level. The sensitivity of these sensors was 23.3 Vs/m, and the range was $\pm 100 \text{ mm/s}$. Acquisition systems were used to record the velocities with a connected laptop computer. The recordings from different sensors were not systematically

synchronized, as the measurements did not contain the same time stamp; rather, the operators at each measurement location started recording based on manual signaling using radio transceivers. Ambient vibration measurements were conducted on the bridge deck under normal traffic conditions and by stopping vehicles over the bridge. Under every type of traffic condition, vibration measurements were conducted for at least 70 s at a sampling rate of 1024 samples per second at all sensors.

3.5 Eigensystem realization algorithm for identifying modal properties

To identify the modal properties of the bridge using the ERA, unsynchronized time history data measured with different sensors were used. To estimate the modal shapes, the cross-correlation [56] was computed between the records from different sensors so that the time lags among the vibrations recorded with different sensors were reduced. The ERA was applied to analyze the vibration time history records. Free vibration data required for the ERA analysis were extracted by selecting decaying portions in the vibration time history data. For the modal analysis, state-space system orders from 2 to 50, which represent the number of modes from 1 to 25 in sequence, were considered (Fig. 7). In general, an identified system consists of true modes and noise modes. At each step of the identification with increasing system order, the poles corresponding to the vibration modes identified at the current system order were compared with the poles identified at the previous lower system order. Stabilization criteria were established to develop a stabilization diagram for distinguishing true modes from noise modes. The stabilization criteria for the modal parameter identification used in this study were as follows: the frequency limit was the relative frequency difference of 1% between the natural frequencies identified at two consecutive system orders, and the damping limit was the relative damping difference between 5% and any identified mode with a Modal Amplitude Coherence (MAC, [46]) value of less than 0.95. Stable frequencies were finally selected from the stabilization diagram based on the stabilization criteria and the Fourier amplitude spectrum (Fig. 7).

3.6 Application of central hinge spring constants in the scour depth estimation

Table 4 presents the spring constants derived after trials following the schemes presented in Figs. 4 and 5 by matching the natural frequency of a particular mode (obtained from the ERA, Sect. 3.5) between the FE model and measurements.

Table 4 Estimated spring constants for the central hinges

Central hinge	E2	E3	E4	E5	E6	E7	E8
Directions	Estimated central hinge spring constants (kN/m)						
x	44,000	54,500	65,000	96,272	148,582	243,893	242,107
y	1649	1656	4674	4796	4674	1656	1649
z	1500	350	700	6460	2115	160	100

Fig. 7 Sample of a stabilization diagram for observation point A at SEC3

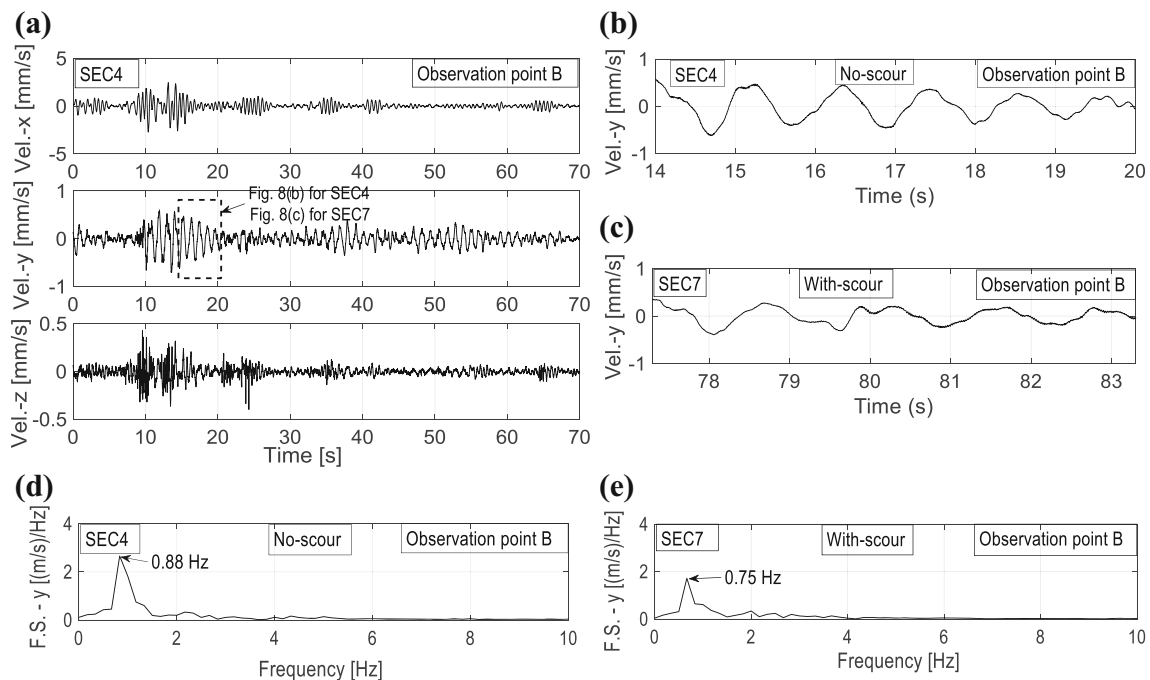
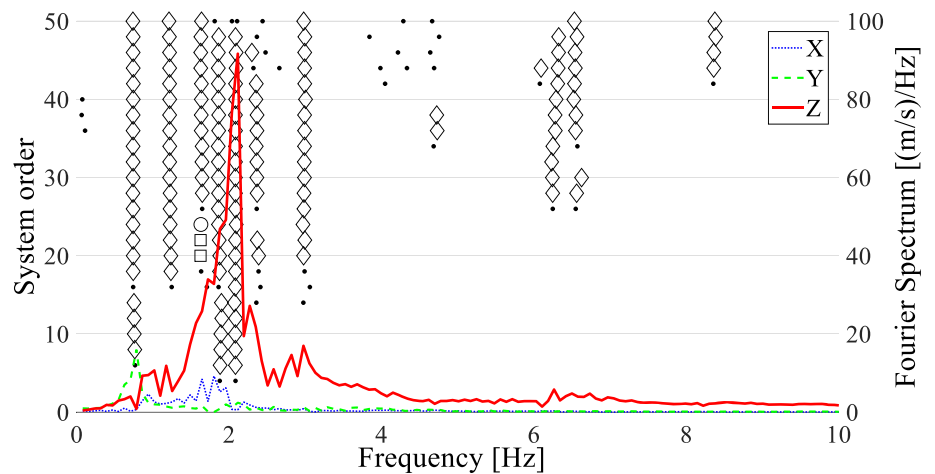


Fig. 8 Evidence of scour observed in free vibration signals and their Fourier spectra. **a** Sample vibration records of SEC4 under ambient conditions, **b** sample free vibration data for SEC4, **c** sample free

vibration data for SEC7, **d** Fourier spectrum of the sample free vibration signal for SEC4, and **e** Fourier spectrum of the sample free vibration signal for SEC7

The ‘Updated FE Model’ with the final central hinge spring constants (Table 4 and Fig. 4) was utilized to derive the generic relation between the scour depth and natural

frequency by simulating scour phenomena and removing soil springs at an interval from the initial riverbed level to estimate the scour depth.

4 Evidence of scour in the vibration measurements

Examples of typical velocity records under ambient conditions are shown in Fig. 8a for ‘no-scour’ and ‘with-scour’ conditions from SEC4 and SEC7 (Pair-II) as a visual comparison to provide preliminary evidence (Fig. 8b, c and see also [15]). The free vibration response reflects the dynamic properties of a structure with a decaying oscillation in the absence of any external forces. The observed free vibration data with a duration of approximately six seconds obtained from field vibration measurements at the superstructure above the pier show that scour increases the period of the signal under the ‘with-scour’ condition compared with that of the signal under the ‘no-scour’ condition due to a reduction in the stiffness. This observation agrees with Prendergast et al. [20, 21]. In addition, a natural frequency shift was observed in the Fourier spectra obtained for the free vibrations under the ‘with-scour’ condition relative to that under the ‘no-scour’ condition; this phenomenon was also due to a loss of stiffness (Fig. 8d, e). The following sections are devoted to transforming these lines of evidence into information regarding an estimation of the scour depth.

5 Modes identified from the field vibration records

Modal analysis was performed on the data in three orthogonal directions obtained from each sensor to obtain the natural frequencies. Subsequently, modal analysis was

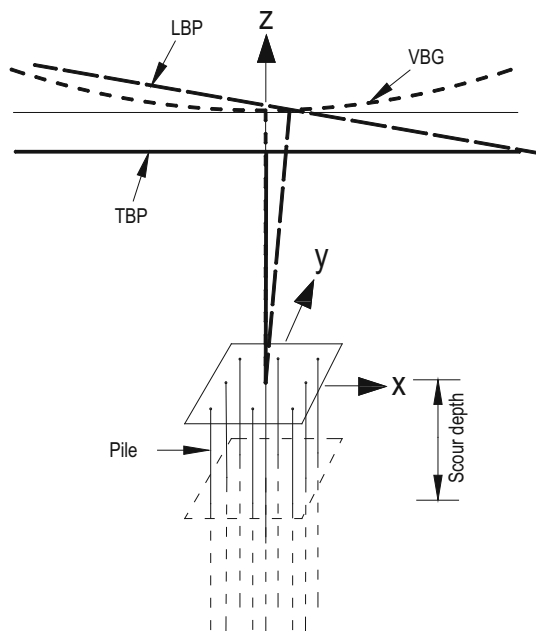


Fig. 9 Mode shapes identified from the analysis

performed on the synchronized data obtained from multiple sensors for each SEC to estimate the mode shapes. However, the modal properties (particularly the phases) identified from synchronized time history data are not always accurate, because synchronization performed by cross-correlation techniques [56] cannot completely synchronize the time histories. In this context, the identified mode shapes were used only to select the natural frequencies of stable vibration modes.

The stable natural frequencies obtained from the vibration time history of each sensor were matched with the natural frequencies obtained from the synchronized time history data, and the corresponding mode shapes were identified. Figure 9 presents the three principal vibration modes selected based on the dominant direction in all data sets. The transverse bending mode of a pier (TBP) represents the bending of the pier in the transverse direction, the longitudinal bending mode of a pier (LBP) represents the bending of the pier in the longitudinal direction in addition to the bending of the girder in the vertical direction, and the vertical bending mode of girders (VBG) represents the bending of the girders in the vertical direction only.

6 Effects of scour on the natural frequency

The natural frequencies of the principal vibration modes obtained from the field vibration data are tabulated for the three pairs of SECs in Table 5. The comparisons between SEC4 and SEC7 (Pair-II) and between SEC5 and SEC6 (Pair-III) show that the natural frequency of the TBP appeared to be lower for SEC7 and SEC6 under the ‘with-scour’ condition than for SEC4 and SEC5 under the ‘no-scour’ condition by 15.7% and 7.7%, respectively. Feng et al. [42], Ju [41], and Prendergast et al. [21] reported through FE analysis; Elsaid and Seracino [35] reported through laboratory experimentation; and Bao et al. [57] reported through both laboratory experimentation and FE analysis that the natural frequencies of transverse and longitudinal bending modes tend to decrease due to a reduction in the flexural stiffness with an increase in the scour depth. In addition, through laboratory experimentation, FE analysis and the field testing of a single pile foundation, Prendergast et al. [44] reported that reductions in natural frequencies occur with increasing scour depth. The difference between the natural frequencies observed for Pair-II and Pair-III may indicate that the free height (including scour) from the girder bottom increased due to scour such that the stiffnesses of SEC7 and SEC6 might have decreased (Table 5). A transverse bending and torsion mode of a pier (TBTP) instead of a TBP was identified for SEC3; a comparison with SEC8 was, therefore, not possible. Usually, when a vibration mode cannot be identified

Table 5 Comparison of the natural frequencies of the principal vibration modes

Vibration mode	Pair-I			Pair-II			Pair-III		
	SEC3 <i>f</i> (Hz)	SEC8	% Difference	SEC4 <i>f</i> (Hz)	SEC7	% Difference	SEC5 <i>f</i> (Hz)	SEC6	% Difference
TBTP	0.74	–	–	–	–	–	–	–	–
TBP	–	0.68	–	0.89	0.75	15.7	0.84	0.77	7.7
LBP	1.87	1.63	12.8	1.84	1.89	– 2.7	1.78	1.85	– 3.9
VBG	2.11	2.11	0	2.01	2.15	– 7.0	2.22	2.27	– 2.3

from field measurement data but the mode can be found in the FE model, it can be taken that these modes are not excited during the measurement. The presence of external and internal disturbances, i.e., noise and water vehicle movement near the measurement location, might be a reason for exciting TBTP mode only at SEC3. Furthermore, the natural frequencies for TBTP and TBP modes in the measurements might be close enough due to any unknown local condition at SEC3 for identification.

In the case of the LBP mode for Pair-I, the natural frequency of SEC8 (with-scour) was lower than that of SEC3 (no-scour) by approximately 12.8% (Table 5). This trend characterizing the relationship between the scour and the natural frequency for Pair-I is similar to that observed in the TBP for Pair-II. However, for the LBP mode for both Pair-II and Pair-III, the natural frequencies of SEC7 and SEC6 were higher by approximately 2.7% and 3.9% than those of SEC4 and SEC5, respectively. For the VBG mode, the natural frequencies of both SECs for Pair-I were the same, and for Pair-II and Pair-III, the natural frequencies for SEC7 and SEC6 were higher than those for SEC4 and SEC5 by approximately 7% and 2.3%, respectively. The VBG results indicate that this mode is not associated with scour; rather, the results are dominated by the dynamic behavior of cantilever part only. The contribution from the substructures should be minor on VBG results.

7 Estimation of the scour depth using the FE model

7.1 Selection of scour-sensitive modes

FE modal analysis was first performed for each SEC considering the boundary conditions at both ends of the cantilever portions as free (Sect. 3.1) representing the condition when the vibration is just initiated from rest. Figure 10 shows the typical mode shapes obtained from the FE analysis along with a comparison of the natural frequencies obtained from the ERA and FE model under free boundary conditions and considering the effects of the central hinge as the boundary condition. The percentage

variation in the natural frequencies ($\Delta\%$) obtained from the ERA and FE model were calculated using the following formula:

$$\Delta(\%) = \frac{f_{ERA} - f_{FEM}}{f_{ERA}} \times 100 \quad (11)$$

For the LBP and VBG modes, the natural frequencies obtained from the measurements were higher than the natural frequencies obtained from the FE analysis by approximately 3–26% for the LBP and approximately 4–11% for the VBG, respectively (Fig. 10, Eq. 11). The discovery of these higher measured natural frequencies indicates a higher stiffness of the SEC, which may be associated with the effects of the central hinges and expansion joint that were neglected in the models at this stage. In the TBP mode, the natural frequencies obtained from the measurements were higher by approximately 4.7% and 8.0% for SEC4 and SEC5, respectively, and lower by approximately – 2.2%, – 14% and – 33.2% for SEC6, SEC7 and SEC8, respectively, than the natural frequencies obtained from the FE analysis (Fig. 10, Eq. 11). The higher measured natural frequencies of the TBP mode for SEC4 and SEC5 can be adjusted by considering the effects of the central hinge. However, for SEC6, SEC7 and SEC8, the lower measured natural frequencies of the TBP mode indicate that these SECs are associated with other forms of damage (especially scour) in addition to that of the central hinge and expansion joints. The natural frequencies of the TBP mode decreased because of the decrease in flexural stiffness with an increase in scour depth. This finding shows the potential of employing the TBP mode for scour detection via comparison with an adequate benchmark.

7.2 Effects of the central hinge on the scour depth estimation

At this stage, the connection in the FE model between two adjacent SECs through a central hinge was simulated by linear springs in the *x*-, *y*- and *z*-directions to increase the natural frequencies of all vibration modes for SEC3, SEC4 and SEC5 under ‘no-scour’ conditions and compared with

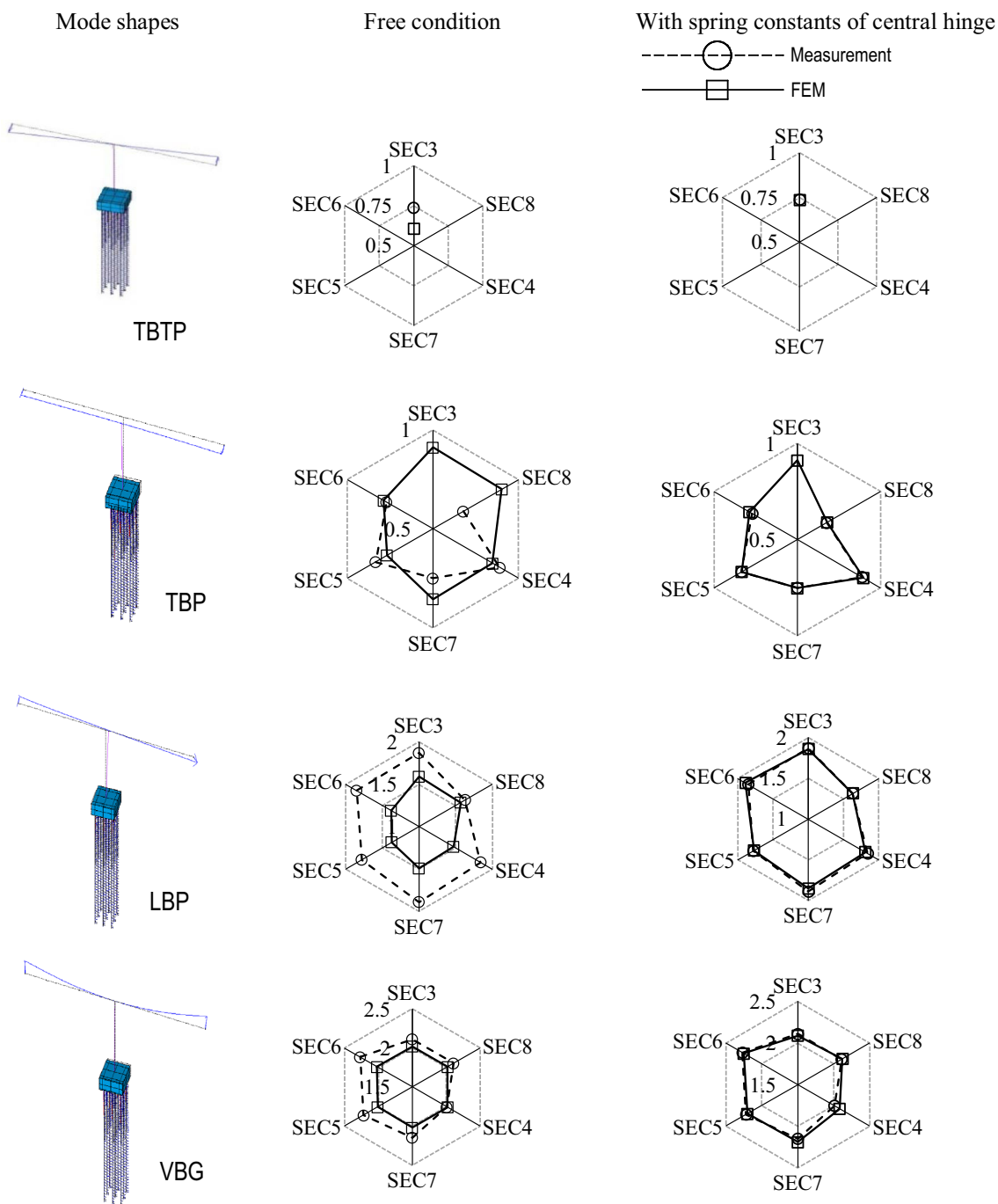


Fig. 10 Comparisons of the natural frequencies (Hz) of the TBTP, TBP, LBP and VBG modes for Pair-I (SEC3 and SEC8), Pair-II (SEC4 and SEC7) and Pair-III (SEC5 and SEC6) obtained from the

ERA and FE model considering free boundary conditions at both ends of the cantilever portions of each SEC and considering the effect of the central hinge as the spring constant

the experimental results (Fig. 4). For SEC6, SEC7 and SEC8, considering the possible effects of scour, only springs in the x - and z -directions were initially added to adjust the natural frequencies of the VBG, which may not be significantly affected by scour. Spring coefficients were adopted in this study through trials to best fit the natural frequencies obtained from the experimental observations

(Table 4). Due to the symmetry of the bridge, the estimated spring constants of the central hinges in the y -direction for SEC3, SEC4 and SEC5 under ‘no-scour’ conditions were used for SEC6, SEC7 and SEC8, respectively, under ‘with-scour’ conditions (first assumption, Sect. 2.1).

Scour was modeled by removing the soil spring step by step from the pile cap bottom. Figure 11 shows the site-

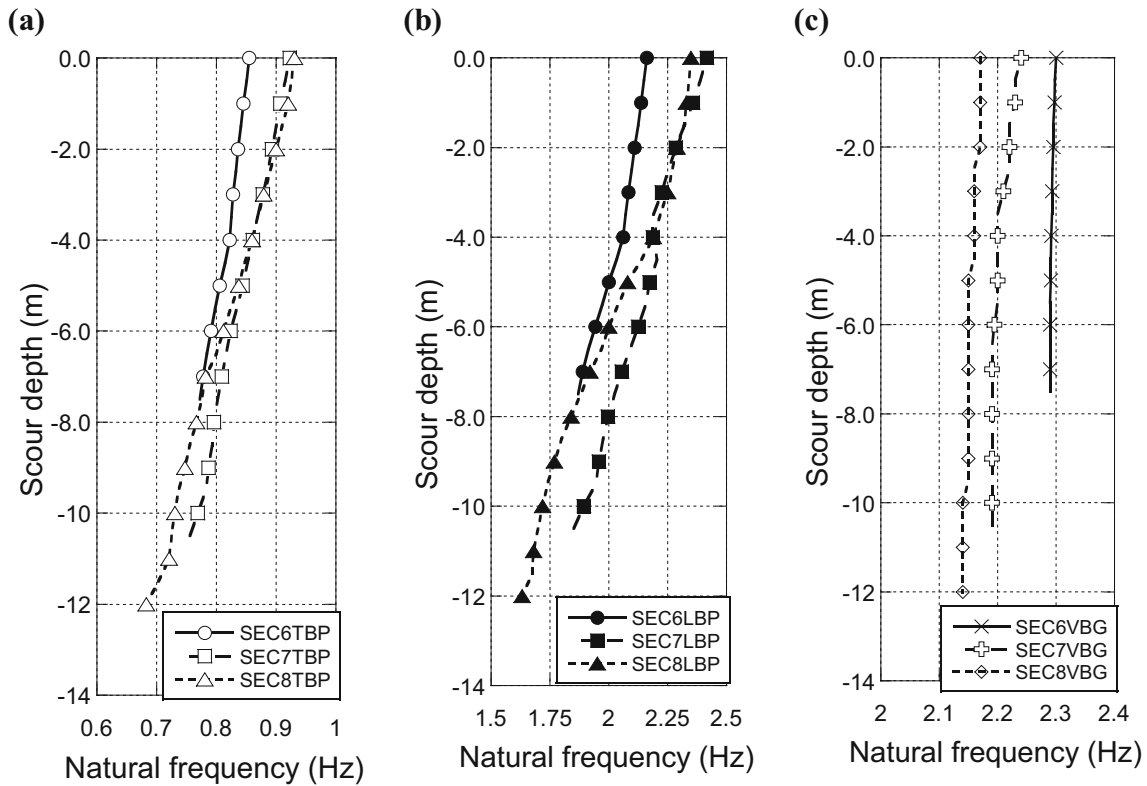


Fig. 11 Comparison of natural frequencies for the three principal vibration modes of a TBP, b LBP, and c VBG with increasing scour depth

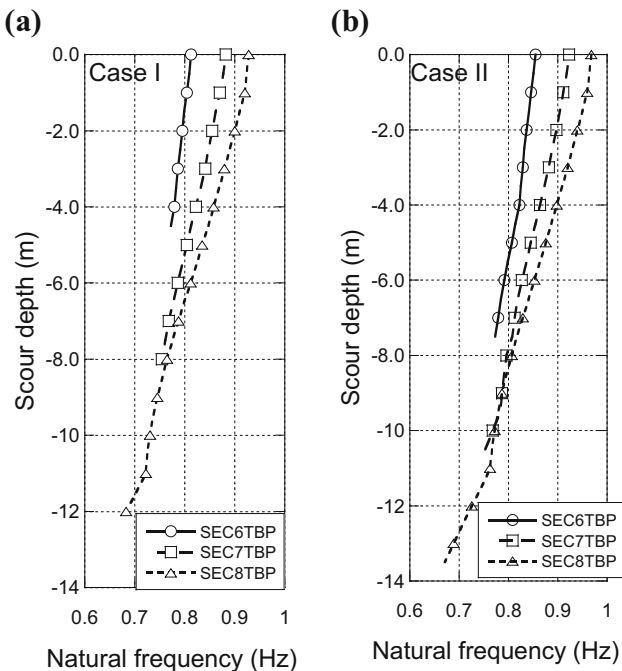


Fig. 12 Changes in the natural frequencies of the TBP mode with increasing scour depth at SEC6, SEC7 and SEC8. a Case I and b Case II

specific changes in the natural frequencies of the three principal vibration modes identified for SEC6, SEC7 and SEC8 due to the increased scour depth at an interval of 0.5 m. Gradual decreases in the natural frequencies of the TBP and LBP modes were observed with increasing scour depth. In contrast, the VBG mode did not have a remarkable correlation with the scour depth, as expected (Fig. 12). A comparison of the natural frequencies obtained after the modification of the boundary conditions in the FE model with the natural frequencies obtained from the ERA is shown in Fig. 10. Because the effects of the central hinges were considered in addition to the simulation of scour, the differences in the natural frequencies were significantly reduced for all SECs, i.e., to less than 3.5% (Eq. 11). For SEC6, SEC7 and SEC8, when the natural frequency of the TBP mode was the closest to the natural frequency obtained from the ERA, the identified scour depths were 7.5, 10.5 and 12.0 m, respectively.

The small gaps (compared with the deflections induced by live traffic loading) between the male and female parts (Table 3) of all central hinges can close under the effects of vibration. To take this into account, two extreme spring constant scenarios in the y-direction were considered for all central hinges (second assumption). Two spring constants in the y-direction, i.e., 1649 kN/m as Case I and 4796 kN/m as Case II (Table 4), were selected based on the minimum

and maximum adopted spring constants of central hinges E2 through E5 for an estimation of the range of scour depths through the updated FE model. A similar procedure was followed to estimate the range of the scour depth. When the natural frequencies of the TBP mode for SEC6, SEC7 and SEC8 obtained from the FE model were closest to the natural frequencies obtained from the ERA, the identified scour depths were, respectively, 4.5, 8 and 12 m for Case I and 7.5, 10.5 and 13.5 m for Case II (Fig. 12). The scour depths estimated for SEC6, SEC7 and SEC8 under the first assumption also lie within the range of scour depths estimated under the second assumption (Sect. 2.1).

Moreover, compared with the free boundary conditions, the correlation between the measurements and FE results in Fig. 10 under closed conditions (Sect. 3.1) indicates that the force causing the dynamic motion of the bridge was strong enough to close the gaps of the central hinge while measuring the vibration.

7.3 Effects of the soil condition on the scour depth estimation

The effects of the soil conditions on the natural frequencies with increasing scour depth were investigated by comparing the simulations of scour under three conditions, i.e., soft soil, hard soil and fixed, using a typical SEC (Fig. 13). The soft soil condition (on the order of $4.0 \times 10^4 \text{ kN/m}^3$) was based on the soil profile at the site (Fig. 3). The Young's modulus of the soil was obtained from Feng et al. [42] using hard soil (on the order of $2.3 \times 10^6 \text{ kN/m}^3$) as a

comparison. Significant differences in the natural frequencies with increasing scour depth were observed under the soft soil condition compared with the hard soil and fixed boundary conditions. This finding justifies the need to consider the soft soil condition in the FE model.

8 Independent verification using bathymetric surveys

The scour depths measured via the echo-sounding technique from three independent surveys [52] were compared for SEC6, SEC7 and SEC8; the estimated scour depth ranges obtained from the FE analysis are shown in Fig. 14. The scour depths estimated through the FE analysis considering the effects of the central hinge range from 12.0 to 13.5 m for SEC8, from 8.0 to 10.5 m for SEC7 and from 4.5 to 7.5 m for SEC6 (Fig. 12); these results are different from those in each of the three surveys (Table 1).

Due to the remnants of earlier protection measures (Sect. 2.2) around the P6, P7 and P8 foundations, it is also valuable to compare the river bed profile transverse to the bridge axis with the vibration-based assessment results. The estimated ranges of the scour depth noted from the bathymetry surveys ranged from 25 to 180 m upstream and 25 to 180 m downstream for SEC8 and SEC7 and from 30 to 100 m upstream and 60 to 160 m downstream for SEC6. However, the locations of the bathymetric survey data were not close to the bridge piers due to turbulence (Sect. 2.2). In general, the maximum scour occurred in the downstream direction due to the eddy currents of the flowing water (Fig. 14). However, in the vicinity of the pier, loose remnants from preceding protection measures (Sect. 2.2) tended to show a spike in the echo-sounding results. However, the numerical model and vibration data provide scour depth information at the centerline because the model and the measured vibration data depend on the stiffness of the bridge pier foundation system associated with the free height (Figs. 1, 2b). Moreover, loose stones from the remnants of earlier mitigation measures do not help in recovering the 'no-scour' design fixity [18]. However, experimental measurements of the scour depth acquired through vibration data can provide a measure of the design fixity [8], whereas echo-sounding bathymetric survey data indicate the distance to a surface from which a sound wave is reflected. These could be a possible reason of discrepancy between the estimates of the scour depths obtained in this study and those from independent bathymetric surveys. The former is more important from a foundation engineering perspective in relation to assuring the stability of the bridge. In this context, the approach presented here provides dependable possibilities for the preliminary detection of scour using vibration data of bridge

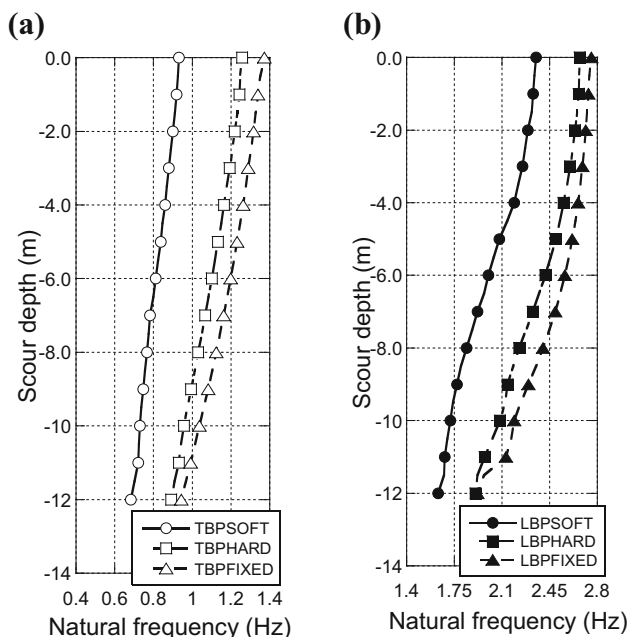


Fig. 13 Effects of the soil condition on the natural frequencies in dominant vibration modes in SEC8. **a** TBP mode and **b** LBP mode

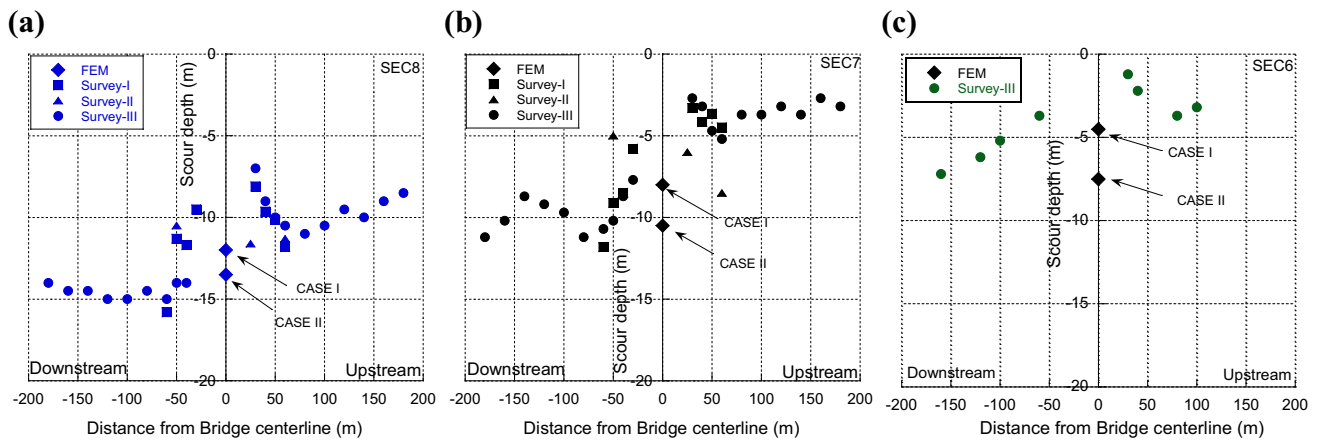


Fig. 14 Comparison of the scour depths under Case I and Case II for **a** SEC8, **b** SEC7 and **c** SEC6

superstructures. The results and discussion herein support that the estimated scour depths obtained in the present study show a reasonable agreement with both field scenarios and engineering considerations. The proposed methodology could be useful for identifying the possible ranges of scour depth before implementing expensive in situ techniques. Moreover, an ideal bridge (implementing an SHM scheme) having baseline (i.e., benchmark) measurements in addition to a scour depth versus natural frequency relation (Figs. 11, 12) for known central hinge conditions can adopt this detection approach more easily and with less computational effort. The gathering of systematic synchronized vibration data will further enhance the detection accuracy coincident with reduced data processing. The thick arrow lines in Fig. 4 delineate such interesting possibilities.

9 Conclusions

To the best of the authors' knowledge, the field testing of real balanced cantilever bridges with central hinges has yet to be performed to estimate the scour depth using vibration data. Accordingly, this study investigated the estimation of the scour depth based on natural frequencies for an existing multi-span PC box girder balanced cantilever bridge exhibiting an actual scour problem in soft soil. The field conditions were more complicated due to the deteriorated performance of the central hinges. A systematic assessment scheme was proposed, verified and discussed for a bridge resting on pile foundations embedded in soft soil with no prior SHM data, which constituted the challenge addressed by this contribution. The following outcomes are noted:

1. The vibration time history data measured from the top of the piers under field conditions were sensitive to scour. Scour was found to increase the period of the

free vibration signals in the time history data and shift the natural frequencies of the signals under 'with-scour' conditions compared with those under 'no-scour' conditions due to a reduction in the stiffness of the pier-pile system.

2. The results of FE analysis demonstrated that the natural frequency of TBP was affected by the presence of scour. Decreases in the natural frequency could be attributed to increases in the free height from riverbed level due to increases in the scour depth, which can reduce the flexural stiffness of the pier. In the experiment, the TBP showed the signs of the effects of scour on natural frequency.
3. The scour depth was reasonably estimated from the natural frequencies of the TBP mode identified from the vibration measurements at the superstructure in combination with the FE model results. The effects of the deteriorated central hinges, through which adjacent structural SECs were dynamically coupled, were considered. The estimated scour depths were in reasonable agreement with the results of independent bathymetric surveys.
4. The significant effects of the soft soil condition on the estimation of the scour depth were examined via a comparison among soft soil, hard soil and fixed boundary conditions in the considered soil-structure interaction model.
5. The results demonstrated the possibility of using the proposed methodology for estimating the scour depth while considering only a single SEC and a few sensors, especially for balanced cantilever bridges with central hinges. The outcomes of the present study supplement the insufficient evidence regarding the applicability of scour depth estimation techniques based on natural frequencies obtained through vibration measurements at the superstructures of real scoured bridges in the literature.

Nonetheless, the field verification of the proposed approach merits application to other balanced cantilever bridges with central hinges, preferably those already constructed, because of its economic advantage and simplicity in regards to its structural design and construction. The proposed approach can be used to estimate the possible range of scour depths in adverse field conditions before performing any expensive (or dangerous, due to river turbulence) in situ scour depth measurement techniques. If possible, future direct field validations could shed light on the sensitivity and reliability of the proposed scheme.

Acknowledgements This research did not receive any specific grant from funding agencies in the public, commercial, or not-for-profit sectors. The authors are grateful to Md. Mashfiqul Islam, Md. Ariful Hasnat, Md. Mahmudul Haque, Nafis Fuad and Md. Abdullah for their enormous support with the vibration measurements. Special thanks are due to the authority of the Bangladesh University of Engineering and Technology for arranging the vehicle used in the vibration measurements. The valuable supports of the Roads and Highways Department of the Government of the People's Republic of Bangladesh, the Corps of Engineers of the Bangladesh Army and the Japan International Co-operation Agency are gratefully acknowledged. Special thanks are owed to Mr. Ryo Tobita, former graduate student, Saitama University, for his valuable support.

References

- Laursen EM, Toch A (1956) Scour around bridge piers and abutments. Iowa Highway Research Board 4, Ames
- Melville BW, Sutherland AJ (1988) Design method for local scour at bridge piers. *J Hydraul Eng* 114:1210–1226. [https://doi.org/10.1061/\(ASCE\)0733-9429\(1988\)114:10\(1210\)](https://doi.org/10.1061/(ASCE)0733-9429(1988)114:10(1210))
- Maddison F (2012) Scour failure of bridges. *Proc ICE-Forensic Eng* 165:39–52. <https://doi.org/10.1680/feng.2012.165.1.39>
- Alam MK, Hasan AKM, Khan MR, Whitney JW (1990) Geological map of Bangladesh: Dhaka. Geological Survey of Bangladesh, scale 1
- Khan FH (1991) Geology of Bangladesh. Wiley Eastern
- Best JL, Ashworth PJ (1997) Scour in large braided rivers and the recognition of sequence stratigraphic boundaries. *Nature* 387:275–277. <https://doi.org/10.1038/387275a0>
- Morgan JP, McIntyre WG (1959) Quaternary geology of the Bengal Basin, East Pakistan and India. *Geol Soc Am Bull* 70:319–342. [https://doi.org/10.1130/0016-7606\(1959\)70\[319:QGOTBB\]2.0.CO;2](https://doi.org/10.1130/0016-7606(1959)70[319:QGOTBB]2.0.CO;2)
- Tomlinson M, Woodward J (2008) Pile design and construction practice. Taylor and Francis Group, USA
- Tappin RGR, Duivendijk JV, Haque M (1998) The design and construction of Jamuna Bridge, Bangladesh. *Proc Inst Civil Engin* 126:150–162
- Sham SHR (2015) Design of the Padma road and rail Bridge, Bangladesh. *Proc Inst Civil Engin* 168:181–192. <https://doi.org/10.1680/bren.14.00029>
- Amin AFMS, Bhuiyan AR, Hossain T, Okui Y (2015) Nonlinear viscosity law in finite-element analysis of high damping rubber bearings and expansion joints. *J Eng Mech*. [https://doi.org/10.1061/\(ASCE\)EM.1943-7889.0000888](https://doi.org/10.1061/(ASCE)EM.1943-7889.0000888)
- Spuler T, Moor G, Ghosh C (2010) Supporting economical bridge construction the central hinge bearings of the 2nd Shitalakshya Bridge. In: Proceedings of the IABSE-JSCE Joint International Conference on Advances in Bridge Engineering-II, International Association for Bridge and Structural Engineering, Zurich, Switzerland/Japan Society of Civil Engineers, Tokyo, pp 275–280
- Wang C, Yu X, Liang F (2017) A review of bridge scour: mechanism, estimation, monitoring and countermeasures. *Nat Hazards*. <https://doi.org/10.1007/s11069-017-2842-2>
- Prendergast LJ, Gavin K (2014) A review of bridge scour monitoring techniques. *J Rock Mech Geotech Eng* 6:138–149. <https://doi.org/10.1016/j.jrmge.2014.01.007>
- Choudhury MSI, Tobita R, Amin AFMS, Matsumoto Y (2015) Experimental investigation on dynamic characteristics of Meghna Bridge at different structural conditions. In: Proceedings of IABSE-JSCE International Conference on Advances in Bridge Engineering-III, Dhaka, Bangladesh, pp 466–475
- Haque MS, Sabur MA, Haider M (2015) Work methodology for replacement of expansion joints of Meghna Bridge in 2008. In: Proceedings of IABSE-JSCE International Conference on Advances in Bridge Engineering-III, Dhaka, Bangladesh, pp 542–548
- Rahman MA, Chong T, Khan MAH (2015) Rehabilitation of Meghna and Meghna-Gumti bridge superstructures. In: Proceedings of IABSE-JSCE International Conference on Advances in Bridge Engineering-III, Dhaka, Bangladesh, pp 510–519
- Noor STN, Amin AFMS, Khan AJ (2015) Numerical investigation of a counter measure to control local scour around a bridge pier: A new source of bridge vibration. In: Proceedings of IABSE-JSCE International Conference on Advances in Bridge Engineering-III, Dhaka, Bangladesh, pp 204–211
- Setia B, Bhatia K (2013) Scour protection by a slot through a model Bridge pier. *J Indian Water Resour Soc* 33:9–15
- Prendergast LJ, Gavin K, Reale C (2016) Sensitivity studies on scour detection using vibration-based systems. *Transp Res Procedia* 14:3982–3989. <https://doi.org/10.1016/j.trpro.2016.05.495>
- Prendergast LJ, Hester D, Gavin K (2016) Determining the presence of scour around bridge foundations using vehicle-induced vibrations. *J Bridge Eng*. [https://doi.org/10.1061/\(ASCE\)BE.1943-5592.0000931](https://doi.org/10.1061/(ASCE)BE.1943-5592.0000931)
- Bao T, Liu Z (2017) Vibration-based bridge scour detection: a review. *Struct Control Health Monit*. <https://doi.org/10.1002/stc.1937>
- Lin YB, Chang KC, Lai JS, Tan YC, Lee FZ (2008) Monitoring scour depth at bridge pier by using MEMS sensors. *Fourth Int Conf Scour Eros* 3:272–275
- Gorin SR, Haeni FP (1989) Use of surface-geophysical methods to assess riverbed scour at bridge piers. Water-Resources Investigations Report 88-4212, U.S. Geological Survey, Hartford, Connecticut, pp 1–33
- Hayes DC, Drummond FE (1995) Use of Fathometers and Electrical-Conductivity Probes to monitor riverbed scour at bridge piers. Water-Resources Investigations Report 94-4164, U.S. Geological Survey, Richmond, Virginia, pp 1–17
- Millard SG, Bungey JH, Thomas C, Soutsos MN, Shaw MR, Patterson A (1998) Assessing bridge pier scour by radar. *NDT E Int* 31:251–258. [https://doi.org/10.1016/S0963-8695\(98\)00006-1](https://doi.org/10.1016/S0963-8695(98)00006-1)
- De Falco F, Mele R (2002) The monitoring of bridges for scour by sonar and sediment. *NDT E Int* 35:117–123. [https://doi.org/10.1016/S0963-8695\(01\)00031-7](https://doi.org/10.1016/S0963-8695(01)00031-7)
- Murrillo JA (1987) The scourge of scour. *Civil Eng ASCE* 57:66–69
- Briaud JL, Ting FCK, Chen HC, Cao Y, Han SW, Kwak KW (2001) Erosion function apparatus for scour rate predictions. *J Geotech Geoenviron* 127:105–113. [https://doi.org/10.1061/\(ASCE\)1090-0241\(2001\)127:2\(105\)](https://doi.org/10.1061/(ASCE)1090-0241(2001)127:2(105))
- Briaud JL, Chen HC, Li Y, Nurtjahyo P, Wang J (2005) SRICOS-EFA method for contraction scour in fine-grained soils. *J Geotech*

- Geoenviron 131:1283–1294. [https://doi.org/10.1061/\(ASCE\)1090-0241\(2005\)131:10\(1283\)](https://doi.org/10.1061/(ASCE)1090-0241(2005)131:10(1283))
31. Wardhana K, Hadipriono FC (2003) Analysis of recent bridge failures in the United States. *J Perform Constr Facil* 17:144–150. [https://doi.org/10.1061/\(ASCE\)0887-3828\(2003\)17:3\(144\)](https://doi.org/10.1061/(ASCE)0887-3828(2003)17:3(144))
 32. Zheng W, Yu W (2014) Probabilistic approach to assessing scoured bridge performance and associated uncertainties based on vibration measurements. *J Bridg Eng*. [https://doi.org/10.1061/\(ASCE\)BE.1943-5592.0000683](https://doi.org/10.1061/(ASCE)BE.1943-5592.0000683)
 33. Choudhury JR, Hasnat A (2015) Bridge collapses around the world: causes and mechanisms. In: Proceedings of IABSE–JSCIE International Conference on Advances in Bridge Engineering-III, Dhaka, Bangladesh, pp 26–34
 34. Foti S, Sabia D (2011) Influence of foundation scour on the dynamic response of an existing bridge. *J Bridg Eng* 16:295–304. [https://doi.org/10.1061/\(ASCE\)BE.1943-5592.0000146](https://doi.org/10.1061/(ASCE)BE.1943-5592.0000146)
 35. Elsaid A, Seracino R (2014) Rapid assessment of foundation scour using the dynamic features of bridge superstructure. *Constr Build Mater* 50:42–49. <https://doi.org/10.1016/j.conbuildmat.2013.08.079>
 36. Lin TK, Wang YP, Huang MC, Tsai CA (2012) 836. Bridge scour evaluation based on ambient vibration. *J Vibroeng* 14:1113–1121
 37. Chen C-C, Wu W-H, Shih F, Wang S-W (2014) Scour evaluation for foundation of a cable-stayed bridge based on ambient vibration measurements of superstructure. *NDT E Int* 66:16–27. <https://doi.org/10.1016/j.ndteint.2014.04.005>
 38. Zarafshan A, Iranmanesh A, Ansari F (2012) Vibration-based method and sensor for monitoring of bridge scour. *J Bridg Eng* 17:829–838. [https://doi.org/10.1061/\(ASCE\)BE.1943-5592.0000362](https://doi.org/10.1061/(ASCE)BE.1943-5592.0000362)
 39. Dutta SC, Roy R (2002) A critical review on idealization and modeling for interaction among soil–foundation–structure system. *Comput Struct* 80:1579–1594. [https://doi.org/10.1016/S0045-7949\(02\)00115-3](https://doi.org/10.1016/S0045-7949(02)00115-3)
 40. Prendergast LJ, Gavin K, Hester D (2017) Isolating the location of scour-induced stiffness loss in bridges using local modal behaviour. *J Civil Struct Health Monit* 7:483–503. <https://doi.org/10.1007/s13349-017-0238-3>
 41. Ju SH (2013) Determination of scoured bridge natural frequencies with soil-structure interaction. *Soil Dyn Earthq Eng* 55:247–254. <https://doi.org/10.1016/j.soildyn.2013.09.015>
 42. Feng CW, Ju SH, Huang HY (2015) Using a simple soil spring model and support vector machine to determine bridge scour depth and bridge safety. *J Perform Constr Facil*. [https://doi.org/10.1061/\(ASCE\)CF.1943-5509.0000837](https://doi.org/10.1061/(ASCE)CF.1943-5509.0000837)
 43. Kong X, Cai CS (2016) Scour effect on bridge and vehicle responses under bridge-vehicle-wave interaction. *J Bridg Eng*. [https://doi.org/10.1061/\(ASCE\)BE.1943-5592.0000868](https://doi.org/10.1061/(ASCE)BE.1943-5592.0000868)
 44. Prendergast LJ, Hester D, Gavin K, O’Sullivan JJ (2013) An investigation of the changes in the natural frequency of pile affected by scour. *J Sound Vib* 332:6685–6702. <https://doi.org/10.1016/j.jsv.2013.08.020>
 45. Pacific Consultants International and Nippon Koei Co. Ltd (1986) Consulting engineering services for the Meghna Bridge construction projects: detail design report
 46. Juang JN, Pappa RS (1985) An eigensystem realization algorithm for modal parameter identification and model reduction. *J Guidance* 8:620–627. <https://doi.org/10.2514/3.20031>
 47. ANSYS14.5 [Computer software]. ANSYS, Canonsburg, PA
 48. Japan International Cooperation Agency, Pacific Consultants International and Nippon Koei Co. Ltd (1998) Basic design study report on the project for protection works for Meghna Bridge in the People’s Republic of Bangladesh
 49. Japan International Cooperation Agency, Pacific Consultants International and Nippon Koei Co. Ltd (1998) Protection works for Meghna Bridge in the People’s Republic of Bangladesh
 50. Japan International Cooperation Agency, Pacific Consultants International and Nippon Koei Co. Ltd (2005) Cross section survey report at Meghna Bridge in the People’s Republic of Bangladesh
 51. Hoque MM, Rahman MM, Hossain MA (2004) Morphological characteristics of the river Meghna: A collaborative study. The 2nd Asia Pacific Association of Hydraulic and Water Resources (APHW) conference, Singapore. <http://rwes.dpri.kyoto-u.ac.jp/~tanaka/APHW/APHW2004/proceedings/FWR/56-FWR-A225/56-FWR-A225.pdf>. Accessed 14 March 2018
 52. Amin AFMS, Matin MA, Amanat KM, Khan AJ, Hoque MS (2012) Scour depth comparisons in the Meghna Bridge, Report. Bureau of research, testing and consultation, Bangladesh University of Engineering and Technology, Dhaka, Bangladesh
 53. Prendergast LJ, Gavin K (2016) A comparison of initial stiffness formulations for small-strain soil–pile dynamic Winkler modelling. *Soil Dyn Earthq Eng* 81:27–41. <https://doi.org/10.1016/j.soildyn.2015.11.006>
 54. Japan Road Association (2002) Japan specifications for highway bridges IV substructures
 55. Bowles LE (1996) Foundation analysis and design. McGraw-Hill, Singapore
 56. MATLAB R2013b [Computer software], MathWorks, U.S
 57. Bao T, Swartz RA, Vitton S, Sun Y, Zhang C, Liu Z (2017) Critical insights for advanced bridge scour detection using the natural frequency. *J Sound Vib* 386:116–133. <https://doi.org/10.1016/j.jsv.2016.06.039>

Publisher’s Note Springer Nature remains neutral with regard to jurisdictional claims in published maps and institutional affiliations.